Leucine-rich repeat transmembrane proteins instruct discrete dendrite targeting in an olfactory map

Weizhe Hong[1], Haitao Zhu[1,4], Christopher J Potter[1], Gabrielle Barsh[1], Mitsuhiko Kurusu[2,3], Kai Zinn[2] & Liqun Luo[1]

Olfactory systems utilize discrete neural pathways to process and integrate odorant information. In *Drosophila*, axons of first-order olfactory receptor neurons (ORNs) and dendrites of second-order projection neurons (PNs) form class-specific synaptic connections at ~50 glomeruli. The mechanisms underlying PN dendrite targeting to distinct glomeruli in a three-dimensional discrete neural map are unclear. We found that the leucine-rich repeat (LRR) transmembrane protein Capricious (Caps) was differentially expressed in different classes of PNs. Loss-of-function and gain-of-function studies indicated that Caps instructs the segregation of Caps-positive and Caps-negative PN dendrites to discrete glomerular targets. Moreover, Caps-mediated PN dendrite targeting was independent of presynaptic ORNs and did not involve homophilic interactions. The closely related protein Tartan was partially redundant with Caps. These LRR proteins are probably part of a combinatorial cell-surface code that instructs discrete olfactory map formation.

Spatial representation of sensory stimuli in the brain is a fundamental organizational principle that facilitates the processing and integration of sensory information[1]. In the visual and auditory systems, neurons connect nearby spatial/frequency inputs to nearby target regions in the brain, thereby forming a spatially continuous neural map. In contrast, the olfactory system utilizes discrete channels to detect olfactory information, with each channel consisting of a group of ORNs that express a specific odorant receptor. The axons of ORNs expressing the same odorant receptor converge on an anatomically discrete glomerular unit in the insect antennal lobe or vertebrate olfactory bulb, the first olfactory processing center in the brain. In each glomerulus, a single class of ORN axons functionally synapses with the dendrites of a single class of second-order olfactory neurons: PNs in insects or mitral cells in vertebrates. Thus, from insects to mammals, olfactory input and output are spatially organized into distinct channels via glomeruli, forming a discrete neural map[1]. Studies of vertebrate visual map formation have supported a crucial role for continuous gradients of guidance molecules for instructing the formation of a continuous neural map during development. However, less is known about the mechanisms by which a discrete map, as exemplified by the olfactory system, is precisely constructed[1,2].

The *Drosophila* antennal lobe consists of ~50 glomeruli, which can be uniquely identified by their stereotypical size, shape and relative position[3]. Most PNs project their dendrites to a single glomerulus and synapse with the axons of a single ORN class. The dendrite targeting of PNs to a specific glomerulus is specified by their lineage and birth order[4]. Notably, the initial targeting of PN dendrites precedes the arrival of pioneering ORN axons[5], suggesting that the coarse glomerular map arises independently of ORN input. The *Drosophila* olfactory system thus provides an attractive model system for studying mechanisms of PN dendrite and ORN axon targeting in the context of discrete map formation.

PN dendrite targeting is presumably achieved by differential expression of cell-surface receptors in different classes of PNs so that they can respond differently to a common environment. Although combinatorial expression of intrinsic transcription factors in PNs has been shown to regulate their dendrite targeting[6–8], little is known about instructive cell-surface receptors during this process. The transmembrane proteins Dscam and N-cadherin are important for the elaboration and refinement of PN dendrites, respectively[9,10], but they are expressed in and required for all PN classes equally. Differential expression of transmembrane Semaphorin-1a regulates coarse dendrite targeting along the dorsolateral-to-ventromedial axis during the initial formation of the antennal lobe[11]. However, no cell-surface molecules have been shown to instruct different classes of PN dendrites to select discrete glomerular targets in a three-dimensional neural map.

We found that the LRR transmembrane protein Caps was differentially expressed in different classes of PNs and cell-autonomously instructed glomerulus-specific targeting of PN dendrites. Further analysis suggested that Caps-mediated dendrite targeting was independent of presynaptic ORNs and did not involve homophilic interactions. We propose that Caps mediates interactions among PN dendrites, leading to a mosaic segregation of Caps-positive and Caps-negative PNs to discrete glomerular targets.

[1]Howard Hughes Medical Institute and Department of Biology, Stanford University, Stanford, California, USA. [2]Division of Biology, California Institute of Technology, Pasadena, California, USA. [3]Structural Biology Center, National Institute of Genetics, and Department of Genetics, the Graduate University for Advanced Studies, Mishima, Japan. [4]Present address: Department of Neurodegeneration, Genentech, South San Francisco, California, USA. Correspondence should be addressed to L.L. (lluo@stanford.edu).

Figure 1 Caps is differentially expressed in the developing antennal lobe. (**a**–**h**) The developing antennal lobes at 48 h APF stained by antibodies against a synaptic marker nc82 (**a**, **d** and **g**), Caps (**b**, **e** and **h**) and *caps-Gal4*–driven mCD8-GFP (**c** and **f**). Caps was differentially expressed in the wild-type developing antennal lobe, as shown in a single anterior (**a**–**c**) and a single posterior section (**d**–**f**) from the same triple-labeled brain. Caps staining was absent in *caps^{c28fs}/Df(3L)Exel6118 trans*-heterozygous mutant antennal lobes (**g**,**h**). (**i**–**k**) Expression of the Flp-out GFP reporter *UAS>stop>mCD8-gfp* at the intersection of *caps-Gal4* and PN-specific *GH146-Flp* in the adult antennal lobe. Three single sections in anterior, central and posterior regions of the antennal lobe are shown (magenta, nc82; green, mCD8-GFP). (**l**) Schematic representation of the glomerular innervation pattern of *caps-Gal4*–expressing PNs across three different sections of the antennal lobe (see **Supplementary Fig. 2** for details). Antennal lobes in this and all subsequent images are shown such that dorsal is up and medial is to the left. Scale bars represent 10 μm.
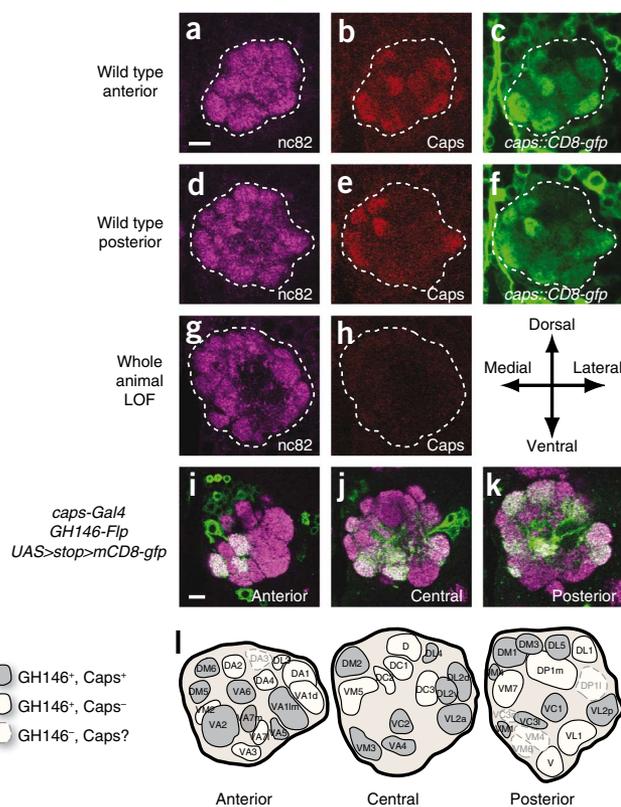
RESULTS

Caps is differentially expressed in different PN classes

To identify instructive cell-surface molecules for PN dendrite targeting, we used a recently established database that contains 976 transmembrane and secreted molecules that are potentially involved in cell-cell recognition[12]. We collected 462 transgenic lines with a UAS insertion in the 5′ end of these genes. These transgenic lines could potentially drive expression of 410 of these 976 genes, covering ~40% of the repertoire of the potential cell-recognition molecules[12]. We expressed each line in a small subset of PNs using *Mz19-Gal4* (ref. 5). We identified P{GS6}10839 in the 5′ end of *caps* as showing a strong PN dendrite mistargeting phenotype.

caps encodes a transmembrane protein with 14 LRRs in its extracellular domain[13]. Previous studies have shown that *caps* is involved in regulating cell-cell interactions in a variety of developmental processes, including boundary formation in wing and leg discs[14,15], organization of the morphogenetic furrow and ommatidial spacing[16], and formation of branch interconnections in tracheal development[17]. In the nervous system, *caps* has been shown to regulate the axon targeting of motor neurons to specific subsets of muscles[12,13] and axon targeting of R8 photoreceptor neurons to the proper layer in the medulla[18].

Staining with polyclonal antibodies to Caps revealed that Caps protein was present in the developing antennal lobe (**Fig. 1a–f** and **Supplementary Fig. 1**). Around 48 h after puparium formation (APF), when individual glomeruli in the antennal lobe are just becoming identifiable, differential Caps expression was evident, with high expression in some glomeruli and low or undetectable expression in others (**Fig. 1b,e**). The distinct expression levels of Caps did not arise from a differential density of neurites, as the density of neurites was rather uniform between different glomeruli, as shown by staining of nc82, a presynaptic marker[19] (**Fig. 1a,d**). The Caps staining was eliminated in a loss-of-function *caps* mutant (**Fig. 1g,h**), indicating that the antibody is specific to endogenous Caps protein. Furthermore, the expression of *UAS–mCD8-gfp* driven by the enhancer trap *caps-Gal4* recapitulated the glomerular-specific Caps staining pattern (**Fig. 1b,c,e,f**), suggesting that *caps-Gal4* is a faithful reporter of endogenous Caps expression.

At 48 h APF, the antennal lobe consists of dendrites from PNs and axons from ORNs. To determine the contribution to *caps* expression by PN dendrites, we generated a PN-specific flipase line, *GH146-Flp*. Similar to the *GH146-Gal4* expression pattern, *GH146-Flp* was expressed in the majority of PNs; these PNs innervated 40 out of the 46 glomeruli that we scored (**Supplementary Fig. 2**). Therefore, we used a Flp-out GFP reporter *UAS>stop>mCD8-gfp* to determine the

intersection of *GH146-Flp* and *caps-Gal4*, and thus Caps expression in PNs (**Supplementary Fig. 2**). Notably, *caps-Gal4* was selectively expressed in a subset of PNs innervating 23 out of 40 *GH146*-positive glomeruli (**Fig. 1i–l** and **Supplementary Fig. 2**). Glomerular targets of Caps-positive and Caps-negative PNs did not segregate into broad domains and appeared to be intercalated (**Fig. 1l**).

Loss of *caps* causes mistargeting of Caps-positive PNs

The differential expression of Caps in different glomeruli raised the possibility that Caps instructs targeting of PN dendrites to specific glomeruli according to Caps expression patterns. This hypothesis predicts that a loss of Caps in Caps-positive PNs should cause their dendrites to mistarget to glomeruli that are normally innervated by Caps-negative PNs, whereas it may not affect the dendrite targeting of Caps-negative PNs. We first tested this prediction by performing mosaic analysis with a repressible marker (MARCM) using the null allele *caps^{c28fs}* for the lateral neuroblast clone containing 12 classes of PNs, nine of which were Caps positive. Loss of *caps* in the lateral neuroblast clones resulted in two types of dendrite targeting defects: loss of innervation in glomeruli that are normally targets of lateral PNs and gain of innervation in glomeruli that are normally not the targets of lateral PNs (**Fig. 2a–c**). In accordance with our prediction, quantitative analysis of dendrite distribution in *caps* mutants showed that all of the glomeruli that exhibited loss of innervation were targets of Caps-positive PNs, whereas the ectopically innervated glomeruli were mostly normal targets of Caps-negative PNs (**Fig. 2d**). This bias of mistargeting toward normal Caps-negative PN targets was highly significant (χ^2, $P < 0.001$; **Supplementary Fig. 3**). Notably, loss of *caps* in Caps-positive PNs did not cause a random mistargeting of dendrites to all Caps-negative targets but instead caused a preferential mistargeting to specific ectopic targets (**Fig. 2d**).

Our analysis of 12 PN classes in neuroblast clones suggests that *caps* is required in PNs for proper dendrite targeting. However, it is

Figure 2 Dendrite targeting phenotypes of *caps*^{−/−} neuroblast clones. (**a**,**b**) Dendrite targeting of neuroblast MARCM clones of wild-type and *caps*^{−/−} PNs. (**a**) Wild-type lateral neuroblast clones stereotypically targeted dendrites to 12 glomeruli. (**b**) *caps*^{−/−} lateral neuroblast clones exhibited selective dendrite mistargeting. The arrowhead indicates the ectopic innervation of VM7, which wild-type PNs do not innervate, and the arrow indicates the loss of innervation of wild-type glomerular target VA4. (**c**) Quantification of dendrite targeting defects in lateral neuroblast MARCM clones of control and *caps* mutant. The *y* axis represents the percentage of the antennal lobes that had mistargeting phenotypes (control, *n* = 9; *caps*^{−/−}, *n* = 12). (**d**) Glomerular innervation specificity of lateral neuroblast MARCM clones of control and *caps* mutants analyzed in **c**. The left 12 columns are the normal glomerular targets of lateral PNs; the green bars represent the percentage of antennal lobes in which an individual glomerulus was innervated and the white bars represent the percentage of antennal lobes in which a normally innervated glomerulus was not innervated. The right 34 columns are glomeruli that are normally not innervated by lateral PNs; the black bars represent the percentage of antennal lobes in which an ectopic glomerulus was innervated. All glomeruli are color coded at the bottom on the basis of expression of Caps in the corresponding PNs as indicated. ND, not determined for Caps expression (*GH146*-negative).
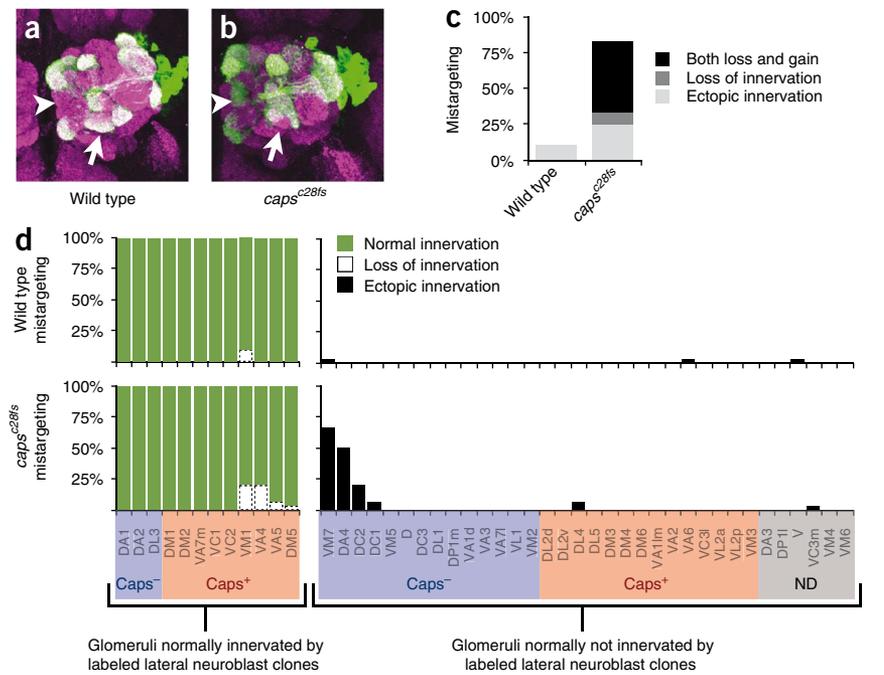
difficult to determine exactly which classes of PNs contribute to the ectopic innervations and whether the loss of innervation is caused by mistargeting rather than by gross defects in dendrite arborization. In addition, it is unclear whether the phenotype is caused by a cell-autonomous requirement for *caps*. To address these questions, we performed MARCM analysis of specific PN classes, including single-cell clones. Using *GH146-Gal4* and *MZ19-Gal4*, along with additional information of neuroblast lineage, heat-shock window and axon-branching pattern, we sampled four Caps-negative (DL1, DA1, DC3 and VA1d) and four Caps-positive (VC1, VC2, VA4 and DM1) PN classes innervating different regions in the antennal lobe (**Fig. 3**, see Online Methods).

Consistent with our prediction, the four Caps-negative PN classes (DL1, DA1, DC3 and VA1d) did not have detectable dendrite targeting defects (**Fig. 3a–c,h–j**). However, loss of *caps* in four Caps-positive PN classes (VC1, VC2, VA4 and DM1) resulted in innervation of additional ectopic glomeruli that were normally targeted by Caps-negative PNs (**Fig. 3d–g,k–n**). All *caps*^{−/−} VC1 PNs exhibited strong ectopic innervation, and 92% of this ectopic innervation occurred in the DA2, DC2, VM7, DC1 and VM5 glomeruli, all of which are normally innervated by Caps-negative PNs (**Fig. 3s,t**). Similarly, loss of *caps* in the Caps-positive VC2, VA4 and DM1 PNs resulted in strong ectopic innervation of the VM7, DA2 and VM5 glomeruli, all of which are normally innervated by Caps-negative PNs (**Fig. 3u,v**). In both cases, the bias of mistargeting toward normal Caps-negative PN targets was highly significant (χ^2, $P < 0.01$; **Supplementary Fig. 3**). Therefore, the loss-of-function analysis in both neuroblast and single-cell clones suggested that Caps instructs the targeting of Caps-positive and Caps-negative PN dendrites to different glomeruli. In the absence of Caps, Caps-positive PNs retained part of their dendrites in their normal glomeruli but mistargeted part of their dendrites preferentially into glomeruli that are normal targets of Caps-negative PNs. We also noticed that *caps*^{−/−} PNs mistargeted to ectopic glomeruli that tended to be in close

proximity to their normal glomerular targets (for example, **Fig. 3w** for VC1), suggesting that Caps regulates local dendrite targeting.

To test the cell autonomy of Caps function, we used MARCM to express a *UAS-caps* transgene only in single cells that were homozygous mutant for *caps* and labeled by mCD8-GFP. This resulted in a rescue of the dendrite mistargeting phenotype of all four Caps-positive PNs (**Fig. 3o–s,u**). Because the *GH146-Gal4* used for rescue was expressed only in postmitotic PNs[8], this result indicates that Caps is cell-autonomously required in postmitotic neurons for the dendrite targeting of these Caps-positive PNs.

In contrast with dendrite mistargeting, lateral horn axon terminal arborization patterns of *caps* mutant PNs still followed their class-specificity, as previously described[20–22] (**Supplementary Fig. 4**, see Online Methods). This suggests that *caps* regulates the targeting of dendrites as opposed to the general fate determination of PNs and that dendrite targeting and axon terminal arborization are separable processes.

Misexpression causes mistargeting of Caps-negative PNs
We found that loss of Caps in Caps-positive PNs caused dendrite mistargeting preferentially to glomerular targets of Caps-negative PNs. Next, we tested whether ectopic expression of Caps in Caps-negative PNs would cause dendrite mistargeting and whether such mistargeting would be preferential to glomeruli that are normally innervated by Caps-positive PNs. We found that MARCM overexpression of Caps in PN neuroblast clones caused severe mistargeting, resulting in a deformation of the entire antennal lobe structure (**Fig. 4a–d**). Next, we misexpressed Caps using *Mz19-Gal4* in three classes of PNs, DA1, VA1d and DC3, which were all Caps negative and sent their dendrites to three adjacent glomeruli (**Fig. 4e,f**). Caps misexpression by *Mz19-Gal4* resulted in a mistargeting of dendrites to nearby VA1lm (81%) and VA4 (31%), both of which were targets of Caps-positive PNs (**Fig. 4f**).

We further misexpressed Caps in a single DL1 PN, which normally did not express (**Fig. 1l**) or require Caps for targeting (**Fig. 3h**).

Figure 3 Cell-autonomous requirement of Caps in Caps-positive PNs for dendrite targeting. (a–c,h–j) Normal dendrite targeting of *caps*^{–/–} MARCM clones in DL1 single cells (h), DA1 neuroblasts (i) and VA1d/DC3 neuroblasts (j), compared with wild type (a–c). These PNs were all Caps negative (*n* = 20 for both wild-type and *caps*^{–/–}). (d–g,k–n) Defective dendrite targeting of VC1, VC2, VA4 and DM1 PNs in single-cell *caps*^{–/–} clones (k–n) compared with wild type (d–g). These PNs were all Caps positive. Their identities were determined as described in the Online Methods. (o–r) Rescue of dendrite targeting of four Caps-positive PNs by expressing a *UAS-caps* transgene only in the single-cell clones. (s–v) Quantification (s,u) and glomerular innervation specificity (t,v) of dendrite targeting defects in single-cell clones of control and *caps* mutant analyzed in d–g and k–r. VC2, VA4 and DM1 were analyzed together (see Online Methods). *y* axes in s and u represent the percentage of PNs in particular classes that have dendrite mistargeting phenotypes. Each black bar in t and v indicates the percentage of antennal lobes in which an ectopic glomerulus was innervated. The glomeruli are color coded as in **Figure 2d**. The VC1 and VC2/VA4/DM1 classes are omitted in t and v, respectively, as they are the ones from which clones were made (wild type: VC1, *n* = 15; VC2, *n* = 15; VA4, *n* = 15; DM1, *n* = 10; *caps*^{–/–}: VC1, *n* = 7; VC2/VA4/DM1, *n* = 19; rescue: VC1, *n* = 6; VC2, *n* = 5; VA4, *n* = 6; DM1, *n* = 4). (w) Schematic representation of the glomerular innervation pattern of individual *caps*^{–/–} VC1 PNs across three different sections of the antennal lobe. Red glomeruli are the ectopic targets of *caps*^{–/–} VC1 dendrites.
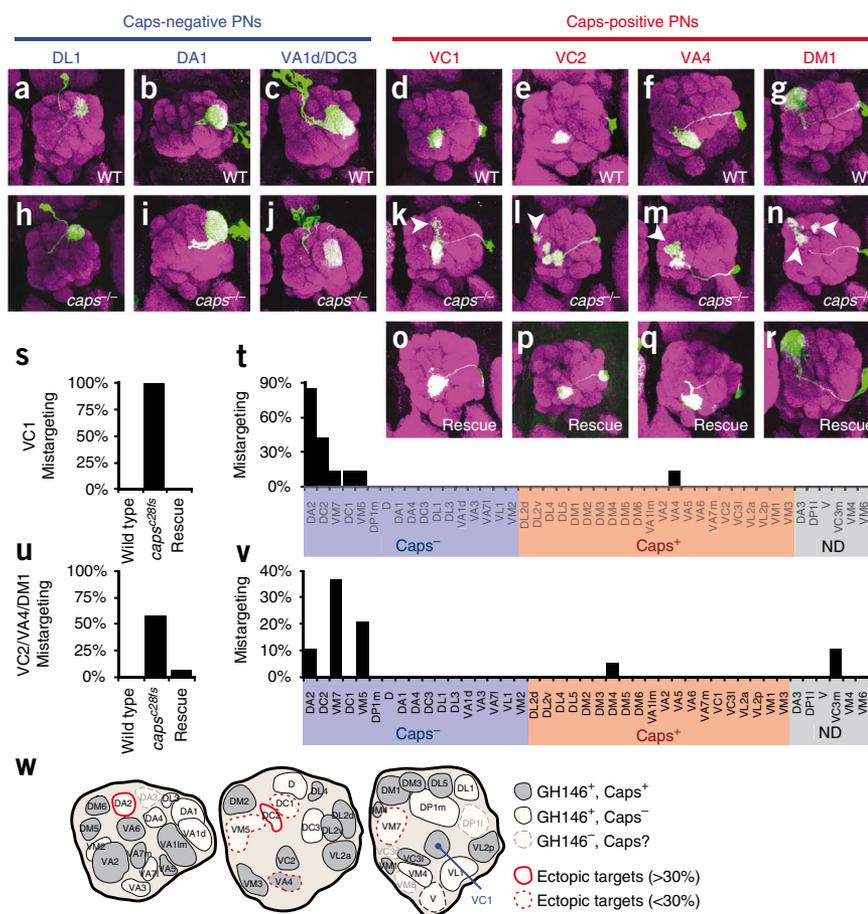
Caps misexpression produced partial loss of innervation of the DL1 glomerulus and ectopic innervation of a selective subset of other glomeruli (**Fig. 4g–i**); these ectopic glomerular targets were normally innervated by Caps-positive PNs, except for DP1l whose Caps expression status was undetermined (**Fig. 4j**). This bias of mistargeting toward normal Caps-positive PN targets was highly significant (χ^2, $P < 0.001$; **Supplementary Fig. 3**), supporting the hypothesis that Caps instructs dendrite targeting of Caps-positive and Caps-negative PNs to different glomeruli. Notably, over two-thirds of the mistargeting events occurred at glomeruli near DL1 (DL2d, DL2v, VL2a and VL2p; **Fig. 4k**), suggesting that mistargeting is preferentially local. We also noticed that mistargeted dendrites avoided two glomeruli DL4 and DL5, which were adjacent to DL1 and innervated by Caps-positive PNs (**Fig. 4k**), suggesting that mistargeting is not random among local ectopic targets (see Discussion). Caps misexpression in single DL1 PNs did not affect PN axon targeting in the lateral horn (**Supplementary Fig. 4**), further confirming that *caps* specifically regulates the specificity of dendrite targeting, as opposed to the general determination of cell fate.

caps is not required for ORN axon targeting

Our expression pattern, loss-of-function and gain-of-function data suggest that Caps instructs dendrite targeting of Caps-positive and Caps-negative PNs to discrete glomeruli. We next explored the cellular mechanisms by which Caps functions to regulate dendrite targeting. Caps has been proposed to determine axon-target connectivity by regulating the interaction between photoreceptor or motor axons and their postsynaptic targets[13,18]. This model is further supported by the recent

observation that Caps appears to mediate direct interaction between postsynaptic filopodia of muscles and presynaptic growth cones[23].

PNs send their dendrites to the developing antennal lobe before the arrival of pioneering ORN axons[5]. The dendrites subsequently elaborate and refine their processes while ORNs extend their axons into the antennal lobe[9,10]. The glomerular positioning of dendrites and axons eventually requires pre- and postsynaptic interactions to achieve the proper matching specificity between PNs and ORNs[9]. If Caps has a function in the olfactory system that is analogous to its role in motor neurons and photoreceptors, it might mediate interactions between ORN axons and PN dendrites. However, the following experiments strongly argue against this model.

To determine whether *caps* is also expressed in presynaptic ORNs, we examined the expression intersection between *caps-Gal4* and *ey-Flp*. *ey-Flp* is expressed in precursors of ORNs but not in central neurons including PNs[24], thereby allowing us to specifically visualize *caps-Gal4* expression in ORNs using a *Flp*-out reporter. We found that *caps-Gal4* was expressed in a subset of ORNs selectively innervating 28 out of 46 glomeruli (**Fig. 5a–d** and **Supplementary Fig. 2**). However, glomeruli innervated by Caps-expressing PNs and ORNs exhibited only partial overlap (**Fig. 5e** and **Supplementary Fig. 2**) and the correlation between Caps expression in PNs and ORNs was not statistically significant (χ^2, $P > 0.3$).

To test whether *caps* is required in ORNs for their axon targeting, we removed *caps* from about half of ORNs using the *ey-Flp* MARCM strategy[24] and analyzed targeting of nine different ORN classes using *Or-Gal4* or *AM29-Gal4* lines to label specific classes of ORN axons. These nine classes of ORN-PN pairs sample four pairs of Caps-positive
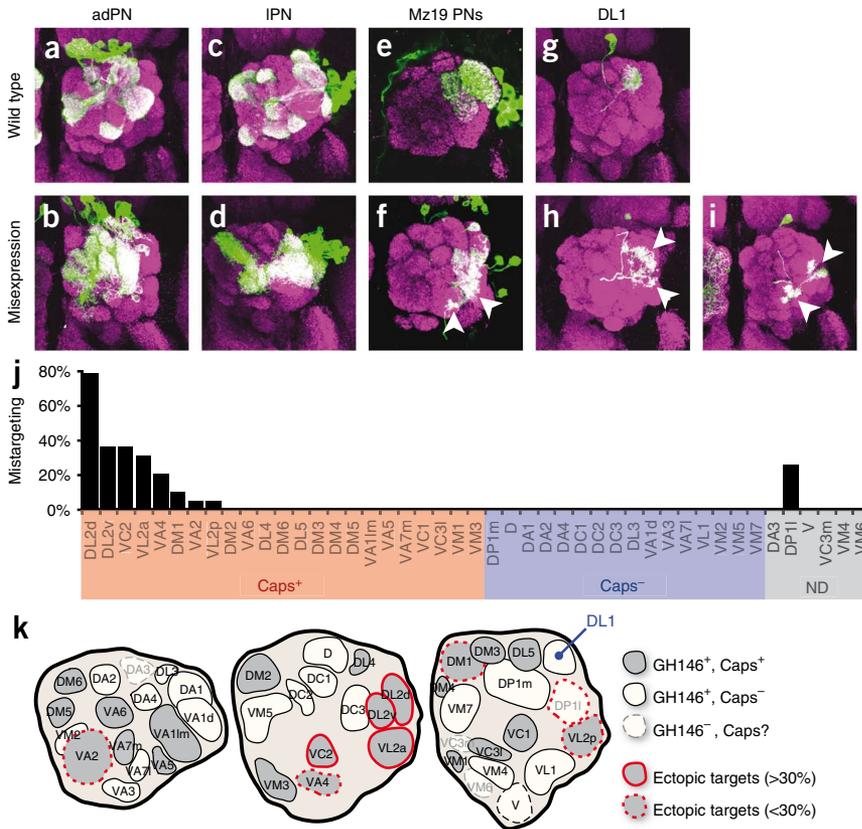
Figure 4 Dendrite targeting phenotypes of Caps misexpression in Caps-negative PNs. (**a–d**) MARCM misexpression of Caps in anterodorsal (**b**) and lateral (**d**) neuroblast clones resulted in severe mistargeting phenotypes compared with wild-type neuroblast clones (**a,c**) (control, $n = 9$; Caps misexpression, $n = 10$). (**e,f**) Caps misexpression in DA1, DC3 and VA1d PNs using *Mz19-Gal4* resulted in strong mistargeting of dendrites to VA1lm and VA4 (arrowheads), both of which were normally innervated by Caps-positive PNs (control, $n = 40$; Caps misexpression, $n = 48$). (**g–i**) Misexpression of Caps in single DL1 PNs using *GH146-Gal4* caused mistargeting of dendrites to ectopic glomeruli (arrowheads in **h** and **i**). (**j**) Quantification of glomerular innervation pattern of individual DL1 PNs misexpressing Caps. Each black bar indicates the percentage of antennal lobes in which an ectopic glomerulus was innervated. All glomeruli are color coded as in **Figure 2d** (control, $n = 20$; Caps misexpression, $n = 19$). (**k**) Schematic representation of the glomerular innervation pattern of individual Caps-misexpressing DL1 PNs across three different sections of the antennal lobe. Red glomeruli indicate ectopic targets of DL1 dendrites misexpressing Caps. adPN, PNs derived from the anterodorsal neuroblast; lPN, PNs derived from the lateral neuroblast.

ORNs and Caps-positive PNs (Or22a-DM2, Or47a-DM3, Or47b-VA1lm and AM29-DM6), four pairs of Caps-positive ORNs and Caps-negative PNs, (Or46a-VA7l, Or59c-VM7, Or67b-VA3 and Or88a-VA1d), and one pair of Caps-negative ORNs and Caps-positive PNs (AM29-DL4). None of these nine ORN classes exhibited any obvious axon-targeting defects (**Fig. 5f–i** and data not shown), indicating that *caps* is not cell-autonomously required in ORNs for their proper axon targeting.

In addition, when the glomerular position of PN dendrites was shifted as a result of the loss of *caps* in ventral VA1lm PNs, the axons of presynaptic Or47b ORNs shifted accordingly without compromising the matching between ORN axons and PN dendrites (**Supplementary Fig. 5**). Thus, loss of Caps in PNs does not appear to disrupt the proper targeting of ORN axons, at least for the specific ORN-PN pair that we tested.

Figure 5 *caps* is not required in ORNs for their axon targeting. (**a–c**) Expression of the intersectional reporter *UAS>stop>mCD8-gfp* for *caps-Gal4* and *ey-Flp*. *ey-Flp* was expressed in ORN precursors but not in PNs or their precursors (magenta, nc82; green, mCD8-GFP). (**d**) Schematic representation of the glomerular innervation pattern of *caps-Gal4*–expressing ORNs across three different sections of the antennal lobe. Gray glomeruli indicate targets of *caps-Gal4*–positive ORNs and white glomeruli indicate targets of *caps-Gal4*–negative ORNs. (**e**) Schematic comparison of the innervation pattern of Caps-positive PNs and ORNs (see also **Supplementary Fig. 2**). (**f–i**) Axon targeting of ORNs in the antennal lobe was not affected in *caps*^{−/−} ORNs. Or67b ORNs innervating VA3 and Or22a ORNs innervating DM2 are shown. In these experiments, only *caps*^{−/−} axons of a particular class of ORNs were visualized by the *Gal4* lines, whereas all of the cells in the central brain, including all PNs, are heterozygous because *ey-Flp* restricts recombination in the olfactory system to the peripheral organs.
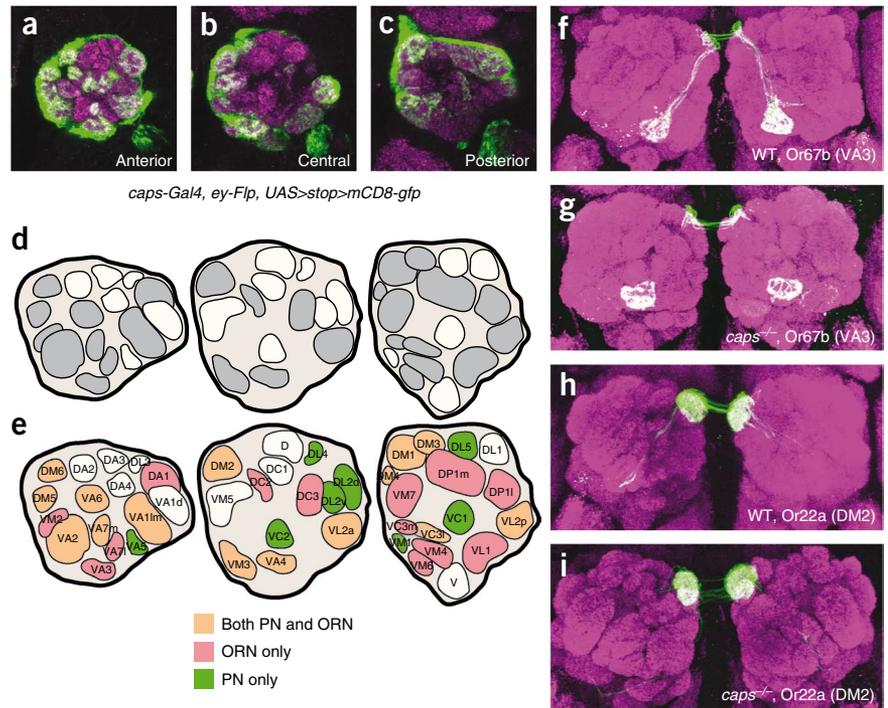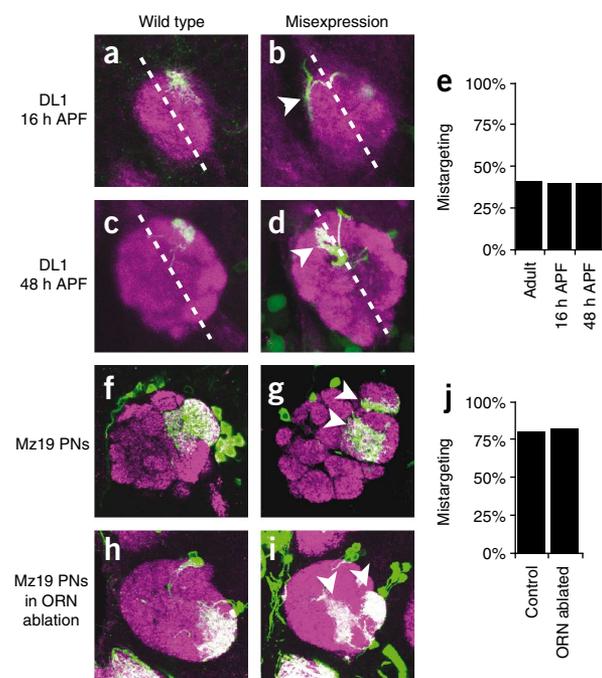
Figure 6 Caps-mediated PN dendrite targeting is independent of ORNs. (**a**–**d**) Mistargeting of DL1 PN dendrites caused by Caps misexpression was observed at early developmental time points. Dotted lines bisect the antennal lobe into dorsolateral and ventromedial parts. Arrowheads in **b** and **d** point to DL1 dendrites that crossed the dotted line and invaded the ventromedial part of the antennal lobe. (**e**) Quantification of mistargeting across the dorsomedial-ventrolateral midline of the antennal lobe (dotted lines in **a**–**d**) at different developmental stages (adult, $n = 12$; 16 h APF, $n = 10$; 48 h APF, $n = 5$). (**f**–**j**) Caps misexpression by *Mz19-Gal4* caused a segregation of dendritic field as a consequence of dendrite mistargeting to VA1lm and VA4 (arrowheads in **g**) compared with continual dendritic field from control *Mz19-Gal4*–labeled PNs (**f**). Caps misexpression by *Mz19-Gal4* in ORN-ablated flies caused dendrite segregation (**i**) compared with control *Mz19* PNs in ORN-ablated flies, which formed a continual field (**h**). (**j**) Quantification of the dendrite segregation phenotypes caused by *Mz19-Gal4* misexpression of Caps, with and without ORN ablation (Caps misexpression without ORN ablation, $n = 48$; Caps misexpression with ORN ablation, $n = 18$).

Caps-mediated PN dendrite targeting is independent of ORNs

Even though Caps is not required for ORN axon targeting, Caps-dependent PN dendrite targeting could, in principle, still depend on the interaction with cues from ORNs. Two lines of evidence argue against the possibility that Caps itself provides the putative ORN-derived cue. First, there was only partial overlap between Caps expression pattern in PNs and ORNs (**Fig. 5e** and **Supplementary Fig. 2**). Second, both loss of innervation and ectopic innervation of PN dendrites occurred in glomerular targets of both Caps-positive and Caps-negative ORNs with no obvious preference (**Supplementary Fig. 3**). These observations argue against a specific hypothesis that PN dendrite targeting is dependent on homophilic interactions of Caps between PN dendrites and ORN axons. Below we provide two lines of evidence further suggesting that Caps-mediated PN dendrite targeting is independent of ORN axons (**Fig. 6**).

We have previously shown that PNs start to elaborate dendrites shortly after puparium formation and that PN dendrites localize to their initial stereotypical target region of the developing antennal lobe before pioneering ORN axons arrive at 18 h APF[5]. Therefore, an examination of dendrites at 16 h APF would allow us to examine the ORN-independent phase of early PN dendrite targeting. Developmental time-course analysis of Caps expression in the antennal lobe indicated that the developing antennal lobe was already positive for both Caps-specific antibody staining and *caps-Gal4* expression at 12–16 h APF (**Supplementary Fig. 1**), confirming that Caps was expressed in developing PN dendrites. At 16 h APF, all wild-type DL1 PN dendrites localized to the dorsal-lateral corner of the developing antennal lobe (**Fig. 6a**); however, Caps misexpression in DL1 caused dendrites to extend across the midline of the dorsomedial-ventrolateral axis of the antennal lobe in ~40% of the samples (**Fig. 6b**), arguing against the possibility that Caps mediates interactions between PN dendrites and ORN axons, at least for PN initial targeting. The medial mistargeting phenotype persisted at 48 h APF (**Fig. 6c,d**) and the penetrance of mistargeting was comparable among different developmental stages (**Fig. 6e**), suggesting that adult defects are likely caused by defects in early PN dendrite targeting.

To further test whether ORN axons are involved in Caps-instructed PN dendrite targeting at a later developmental stage, we compared Caps misexpression phenotypes in an otherwise normal or ORN-ablated background. If Caps instructs PN dendrite targeting by mediating the interactions between ORN axons and PN dendrites, we expect that ORN ablation would suppress the mistargeting phenotypes of PN dendrites caused by PN misexpression of Caps. To ablate all ORNs during early development, we used *Pebbled-Gal4* and *ey-Flp* to express the flip-out toxin *UAS>stop>RicinA*. *Pebbled-Gal4* and

ey-Flp are expressed in all ORNs during early development[24] and this strategy therefore ablated almost all ORNs before their axons entered the developing antennal lobe (**Supplementary Fig. 6**). *ey-Flp* is not expressed in PNs or their progenitors, allowing us to simultaneously use a PN–specific *Mz19-Gal4* line to assess PN dendrite development in ORN-ablated flies.

Mz19-Gal4 labeled three PN classes innervating three adjacent glomeruli, DA1, VA1d and DC3, located in the dorsolateral region of the antennal lobe (**Fig. 6f**). When ORNs are ablated during development, the dendrites of these three PN classes still converged to discrete regions and remained adjacent to each other, although they were located in the ventrolateral region as a result of a shift of the antennal lobe orientation in the absence of ORN axons (**Fig. 6h**). These results suggest that PNs retain their intrinsic ability to converge their dendrites to specific glomerular regions at both early and late developmental stages without the contribution of ORN axons. Caps misexpression by *Mz19-Gal4* resulted in mistargeting of PN dendrites to VA1lm and VA4 and the dendrites were frequently segregated to nonadjacent regions in the antennal lobe as a consequence of this mistargeting (**Fig. 6g**). Notably, this dendrite segregation also occurred when Caps was misexpressed by *Mz19-Gal4* after ablating all ORNs (**Fig. 6i**), and the penetrance was comparable to Caps misexpression without ORN ablation (**Fig. 6j**).

Taken together, these data strongly suggest that Caps instructs PN dendrite targeting independently of ORN axons throughout development. Besides ORNs, PNs are likely the only cell type that can provide class-specific positional cues. Given the mosaic distribution of Caps-positive and Caps-negative glomeruli, we suggest that Caps regulates PN dendrite targeting through PN-PN interactions, as opposed to responding to a global cue, leading to a segregation of Caps-positive and Caps-negative PNs to different glomeruli (see Discussion).

Caps does not mediate homophilic interactions

Caps has been proposed to act as a homophilic recognition molecule on the basis of its ability to promote S2 cell aggregation, although this can only be seen when the expression level is very high[13,14,18] (A. Nose, personal communication). Here, we used a genetic approach

Figure 7 Caps does not mediate homophilic interactions for PN dendrite targeting. (**a**) Normal dendrite targeting of a single DL1 PN in a *caps* whole-animal mutant (*caps^c28fs/Df(3L)Exel6118*). (**b,c**) Dendrite mistargeting of a single DL1 PN misexpressing Caps in an otherwise wild-type background (**b**) or an otherwise *caps^c28fs/Df(3L)Exel6118* mutant background (**c**). (**d**) Quantification of DL1 targeting defects for the genotypes in **a**–**c**. (DL1 labeling in wild-type background, *n* = 20; DL1 labeling in *trans*-heterozygous mutant background, *n* = 20; Caps misexpression in an otherwise wild-type background, *n* = 8; Caps misexpression in an otherwise *trans*-heterozygous mutant background, *n* = 9). Gray bars represent the percentage of partial mistargeting events in which PN dendrites still partially innervated DL1, and black bars represent the percentage of full mistargeting events in which no dendrites innervated DL1.
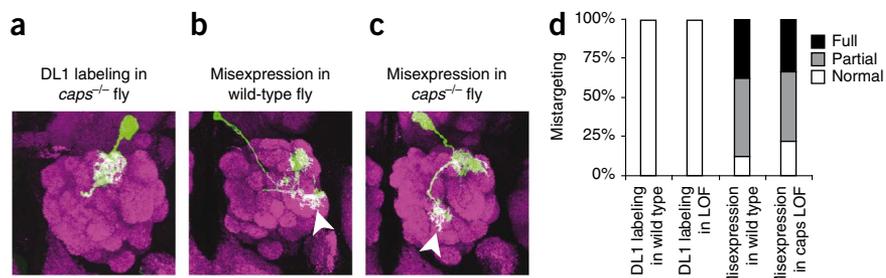
to functionally test whether Caps mediates homophilic interactions *in vivo* during PN dendrite targeting (**Fig. 7**). We found that Caps misexpression in a single Caps-negative DL1 PN resulted in a preferential mistargeting (**Fig. 4h,i** and **7b**). If homophilic interactions among Caps-expressing cells underlie this misexpression phenotype, we would expect that eliminating endogenous Caps expression in the entire fly would suppress this phenotype.

The *caps* homozygous mutants die primarily as embryos, but a few (<0.1%) survive until adulthood. DL1 PN dendrites still targeted properly to the DL1 glomerulus in these *caps* homozygous mutants (**Fig. 7a**). However, ectopic expression of Caps in a single DL1 PN in these *caps* mutant flies still caused mistargeting of DL1 dendrites to ectopic glomeruli in the antennal lobe (**Fig. 7c**). Quantification

showed that Caps misexpression in single DL1 PN caused a similar degree of mistargeting in a whole-animal *caps^−/−* background as in the wild type (**Fig. 7d**), indicating that Caps-dependent dendrite targeting does not use Caps in other cells as a cue, at least in the gain-of-function context. Overall, these data suggest that Caps uses a heterophilic ligand to instruct dendrite targeting.

Partially redundant function of Caps and Tartan

Caps shares 67% sequence identity in its extracellular domain with another LRR transmembrane protein, Tartan (Trn)[13,25], the closely related paralog of Caps. *trn* and *caps* have redundant functions in regulating boundary formation in wing imaginal dics[14,26], leg segmentation[15] and the architecture of the morphogenetic furrow and ommatidial spacing[16]. In the nervous system, *trn* and *caps* also have redundant functions in regulating motor axon targeting[12,23]. Indeed, Trn overexpression also resulted in dendrite mistargeting phenotypes in
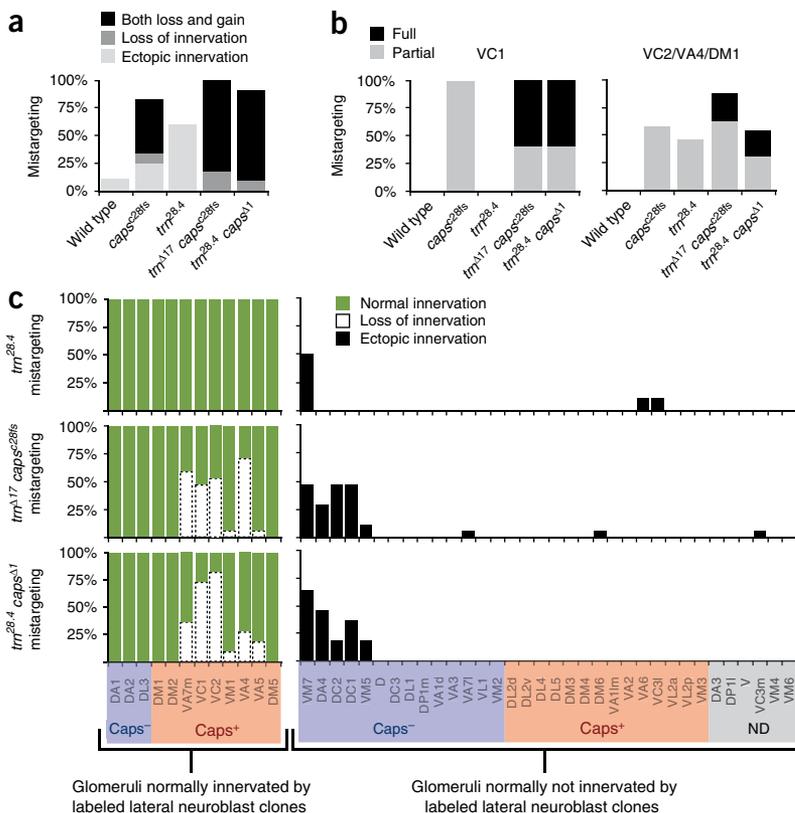

Figure 8 *trn* enhances *caps* phenotypes in PN dendrite targeting. (**a**) Quantification of dendrite targeting defects in lateral neuroblast MARCM clones of control, single and double mutants of *caps* and *trn*, as indicated. The *y* axis and the colored bars are represented as described in **Figure 2c** (wild type, *n* = 31; *caps^c28fs FRT2A*, *n* = 30; *trn^28.4 FRT2A*, *n* = 18; *trn^Δ17 caps^c28fs FRT2A*, *n* = 17; *trn^28.4 caps^Δ1 FRT80B*, *n* = 11). (**b**) Quantification of dendrite targeting defects in single-cell MARCM clones of control, single and double mutants of *caps* and *trn*, as indicated. The *y* axis and the bars are represented as described in **Figure 7d** (for VC1, wild type, *n* = 20; *caps^c28fs FRT2A*, *n* = 7; *trn^28.4 FRT2A*, *n* = 5; *trn^Δ17 caps^c28fs FRT2A*, *n* = 5; *trn^28.4 caps^Δ1 FRT80B*, *n* = 5; for VC2/VA4/DM1, wild type, *n* = 30; *caps^c28fs FRT2A*, *n* = 19; *trn^28.4 FRT2A*, *n* = 13; *trn^Δ17 caps^c28fs FRT2A*, *n* = 16; *trn^28.4 caps^Δ1 FRT80B*, *n* = 13). (**c**) Glomerular innervation specificity of the lateral neuroblast MARCM clones of *trn* single mutant and *trn caps* double mutants analyzed in **a**. The *y* axis and the colored bars are represented as described in **Figure 2d**. (**d–h**) Dendrite targeting of single-cell VC1 MARCM clones of control, single and double mutants of *caps* and *trn*, as indicated. Arrowheads indicate the ectopic innervation of DA2, which wild-type VC1 PNs did not innervate.
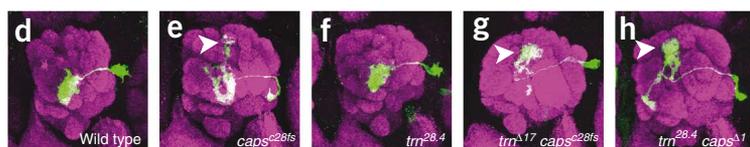
neuroblast clones and DL1 single PN clones (**Supplementary Fig. 7**). Moreover, the expression of an enhancer trap *trn-lacZ*, along with *caps-Gal4*, *GH146-Flp* and *UAS>stop>mCD8gfp*, indicated that *trn* was expressed in PNs and partially overlapped with *caps* expression (**Supplementary Fig. 7**).

To test the requirement of *trn* in PN dendrite targeting and its potential redundant function with Caps, we carried out loss-of-function studies of *trn* single and *trn caps* double mutants, analogous to the *caps* experiments described above (**Fig. 8**). We found that the loss of *trn* in the lateral neuroblast clone resulted only in ectopic innervation, but two independent *trn caps* double-mutant pairs showed a significantly higher percentage of combined loss of innervation and ectopic innervation compared with either of the single mutants (**Fig. 8a**). A glomerulus is usually innervated by multiple PNs so that ectopic innervation reflects a partial mistargeting of these PNs, whereas loss of innervation indicates that all of these PNs completely mistarget away from the normal region. The loss of innervation of VA7m, VC1 and VC2 were not observed in either *caps* (**Fig. 2d**) or *trn* single mutants but occurred frequently in *trn caps* double mutants (**Fig. 8c**), indicating that *trn caps* double mutants have more severe mistargeting phenotypes. Furthermore, single-cell loss-of-function analysis of VC1 and VC2/VA4/DM1 PNs consistently revealed more severe mistargeting phenotypes for double mutants than for either of the single mutants (**Fig. 8b**). For example, *caps* single-mutant VC1 PNs always retained a part of their dendrites in the VC1 glomerulus (**Fig. 8b,e**); however, a large percentage of *trn caps* double-mutant VC1 PNs no longer innervated VC1 at all (**Fig. 8b,g,h**), consistent with the strong loss of innervation of VC1 that we observed in lateral neuroblast clones of *trn caps* double mutants. Given that Caps and Trn have high sequence similarity, similar overexpression phenotypes, overlapping expression patterns and enhancement of PN dendrite mistargeting in double mutants compared with either of the single mutants alone, we conclude that Caps and Trn have partially redundant functions in PN dendrite targeting. However, similar to the *caps* single mutant, neither *trn* single nor *trn caps* double mutants had any obvious targeting defects in the axons of nine different ORN classes tested for *caps* single mutants (data not shown), suggesting that Trn and Caps are dispensable for ORN axon targeting.

DISCUSSION

Discrete cell-surface codes in a discrete neural map

Graded expression of guidance molecules is widely used in patterning continuous, topographic representation of sensory inputs. A classic example is graded Ephrin/Eph signaling in regulating retinotopic projections in vertebrates[1,27]. Graded molecules may also be used in the initial coarse patterning of discrete olfactory maps in flies and mice[11,28], but selective targeting to discrete glomerular units requires additional mechanisms. Here, we found that the LRR transmembrane protein Caps was expressed in a subset of PNs whose dendrites targeted to a subset of glomeruli intermingled with other glomeruli targeted by Caps-negative PNs. Loss of *caps* selectively affected targeting of Caps-positive PNs, causing them to preferentially mistarget to glomeruli that were normally innervated by Caps-negative PNs. Conversely, misexpression of Caps in Caps-negative PNs caused them to selectively target dendrites to glomeruli that are normal targets of Caps-positive PNs. These data indicate that Caps instructs the targeting of Caps-positive and Caps-negative PN dendrites to discrete glomeruli in the *Drosophila* antennal lobe.

How does Caps-mediated targeting act together with molecular gradients used for establishing the coarse dendrite map? A general conceptual problem of making a discrete map using gradient cues is that nearby discrete glomerular units have to be distinguished with a minimal difference in gradient cues. One potential solution would be to express a second type of cell-surface molecules that form a spatially intercalated expression pattern with a tight correlation with each discrete class of neurons. Indeed, recent studies in mouse ORN axon targeting have suggested a hierarchical model in which molecular gradients help coarse targeting of axons, followed by local refinement mediated by activity-dependent expression of cell-recognition molecules[1,2]. Neuropilin-1 and Semaphorin-3A are expressed in broad domains in olfactory bulb and disruption of Semaphorin-3A causes global axon mistargeting[29–33]. However, other cell-surface molecules, including Ephrin-A2/A5 and EphA5, as well as immunoglobulin superfamily proteins Kirrel-2, Kirrel-3 and BIG-2, are differentially expressed in a mosaic pattern and likely regulate local axon targeting through axon-axon interactions among ORNs[34–36].

Drosophila PN dendrite targeting appears to utilize a conceptually similar strategy even though details may differ regarding types of molecules, cells (ORNs versus PNs), neuronal processes (axons versus dendrites) and dependence on activity; this hierarchical regulation may be a general strategy for discrete map formation. Specifically, we propose that molecular gradients such as Semaphorin-1a may set up a coarse map for PN dendrites. This is followed by Caps-dependent local dendrite targeting to discrete glomeruli. In support of this notion, loss of *semaphorin-1a* causes a directional shift of dendrites[11], whereas loss of *caps* causes a specific mistargeting to local ectopic targets.

Both loss-of-function and misexpression analyses indicate that the mistargeted dendrites are restricted to only a subset of ectopic glomeruli following the Caps code. For example, Caps-misexpressing DL1 PNs mistargeted to the DL2v and DL2d glomeruli but avoided DL4 and DL5 glomeruli, even though they were all in the vicinity of DL1 and were normal targets of Caps-positive PNs. Similarly, *caps* loss of function in VC1 PNs caused dendrites to mistarget to VM7, DC2, DC1 and VM5, and to avoid VL1, DP1m and DC3, even though they were all in the vicinity of VC1 and were normal targets of Caps-negative PNs. These observations suggest that additional molecules must work together with Caps to distinguish targeting specificity among different Caps-positive PNs or among different Caps-negative PNs. Because these additional molecules are still intact in PNs with an altered Caps code, their actions might explain the mistargeting specificity. Thus, Caps likely acts in parallel with additional molecules to specify dendrite targeting of the 50 PN classes into areas that eventually develop into 50 glomeruli.

Cellular and molecular mechanisms

The matching expression of Caps in motor neurons and their target muscles[12,13], as well as in R8 photoreceptor axons and their target layers[18], suggest that Caps functions in synaptic matching through interactions between pre- and postsynaptic partners. During the assembly of the olfactory system, 50 classes of ORN axons need to match with 50 classes of PNs. However, our data strongly argue against the possibility that the PN dendrite targeting defect is caused by a predominant role of Caps in mediating synaptic matching between ORN axons and PN dendrites. First, *caps* is required for targeting of PN dendrites but not ORN axons. This cannot be caused by the redundancy with its close paralog Trn, as *trn caps* double mutants enhanced *caps* phenotypes in PN dendrite targeting but still exhibited no phenotypes in ORNs. Second, expression patterns of Caps in PNs and ORNs did not match with regard to their glomerular targets. Third, Caps-mediated PN dendrite targeting was independent of ORNs. Fourth, Caps misexpression phenotype was not affected by

1549

the loss of Caps in all other cells, suggesting that it interacts with a heterophilic ligand for PN dendrite targeting.

The use of a heterophilic ligand is consistent with studies of Caps in boundary formation of the wing imaginal disc[14,26]. Given the mosaic distribution of Caps-positive and Caps-negative glomeruli, as well as the similarities with the axon-axon interactions in refining local targeting of mouse ORN axons, we propose that the heterophilic Caps ligand is most likely derived from other PNs and that the interactions between Caps and its ligand mediate PN-PN interactions to segregate Caps-positive and Caps-negative PNs to specific glomeruli.

How do Caps and its heterophilic ligand segregate Caps-positive and Caps-negative PNs via PN-PN interactions? The simplest hypothesis consistent with our data is that a repulsive ligand is expressed in Caps-negative PNs, forming a mosaic pattern complementary to Caps. Caps and its ligand mediate repulsive interactions among PN dendrites to segregate Caps-positive and Caps-negative PNs. When Caps is lost in a Caps-positive PN, its dendrites innervate ectopic glomeruli that are preferentially targets of Caps-negative PNs because of a loss of repulsion from Caps-negative PN dendrites; additional molecules that normally instruct Caps-positive PN dendrites to select a specific Caps-positive glomeruli are still intact, thereby preventing *caps* mutant PNs from invading other Caps-positive glomeruli. When Caps is misexpressed in a Caps-negative PN, the repulsive ligand would force dendrites to mistarget to glomerular targets of Caps-positive PNs. Future identification of the Caps ligand will be essential to test this hypothesis and will shed further light on the mechanisms of discrete olfactory map formation.

METHODS

Methods and any associated references are available in the online version of the paper at http://www.nature.com/natureneuroscience/.

Note: Supplementary information is available on the Nature Neuroscience website.

1. Luo, L. & Flanagan, J.G. Development of continuous and discrete neural maps. *Neuron* **56**, 284–300 (2007).
2. Imai, T. & Sakano, H. Roles of odorant receptors in projecting axons in the mouse olfactory system. *Curr. Opin. Neurobiol.* **17**, 507–515 (2007).
3. Laissue, P.P. *et al.* Three-dimensional reconstruction of the antennal lobe in *Drosophila melanogaster*. *J. Comp. Neurol.* **405**, 543–552 (1999).
4. Jefferis, G.S., Marin, E.C., Stocker, R.F. & Luo, L. Target neuron prespecification in the olfactory map of *Drosophila*. *Nature* **414**, 204–208 (2001).
5. Jefferis, G.S. *et al.* Developmental origin of wiring specificity in the olfactory system of *Drosophila*. *Development* **131**, 117–130 (2004).
6. Komiyama, T., Johnson, W.A., Luo, L. & Jefferis, G.S. From lineage to wiring specificity. POU domain transcription factors control precise connections of *Drosophila* olfactory projection neurons. *Cell* **112**, 157–167 (2003).
7. Komiyama, T. & Luo, L. Intrinsic control of precise dendritic targeting by an ensemble of transcription factors. *Curr. Biol.* **17**, 278–285 (2007).
8. Spletter, M.L. *et al.* Lola regulates *Drosophila* olfactory projection neuron identity and targeting specificity. *Neural Dev.* **2**, 14 (2007).
9. Zhu, H. *et al.* Dendritic patterning by Dscam and synaptic partner matching in the *Drosophila* antennal lobe. *Nat. Neurosci.* **9**, 349–355 (2006).
10. Zhu, H. & Luo, L. Diverse functions of N-cadherin in dendritic and axonal terminal arborization of olfactory projection neurons. *Neuron* **42**, 63–75 (2004).
11. Komiyama, T., Sweeney, L.B., Schuldiner, O., Garcia, K.C. & Luo, L. Graded expression of semaphorin-1a cell-autonomously directs dendritic targeting of olfactory projection neurons. *Cell* **128**, 399–410 (2007).
12. Kurusu, M. *et al.* A screen of cell-surface molecules identifies leucine-rich repeat proteins as key mediators of synaptic target selection. *Neuron* **59**, 972–985 (2008).
13. Shishido, E., Takeichi, M. & Nose, A. *Drosophila* synapse formation: regulation by transmembrane protein with Leu-rich repeats, CAPRICIOUS. *Science* **280**, 2118–2121 (1998).
14. Milán, M., Weihe, U., Pérez, L. & Cohen, S.M. The LRR proteins capricious and Tartan mediate cell interactions during DV boundary formation in the *Drosophila* wing. *Cell* **106**, 785–794 (2001).
15. Sakurai, K.T., Kojima, T., Aigaki, T. & Hayashi, S. Differential control of cell affinity required for progression and refinement of cell boundary during *Drosophila* leg segmentation. *Dev. Biol.* **309**, 126–136 (2007).
16. Mao, Y., Kerr, M. & Freeman, M. Modulation of *Drosophila* retinal epithelial integrity by the adhesion proteins capricious and tartan. *PLoS One* **3**, e1827 (2008).
17. Krause, C., Wolf, C., Hemphälä, J., Samakovlis, C. & Schuh, R. Distinct functions of the leucine-rich repeat transmembrane proteins capricious and tartan in the *Drosophila* tracheal morphogenesis. *Dev. Biol.* **296**, 253–264 (2006).
18. Shinza-Kameda, M., Takasu, E., Sakurai, K., Hayashi, S. & Nose, A. Regulation of layer-specific targeting by reciprocal expression of a cell adhesion molecule, capricious. *Neuron* **49**, 205–213 (2006).
19. Wagh, D.A. *et al.* Bruchpilot, a protein with homology to ELKS/CAST, is required for structural integrity and function of synaptic active zones in *Drosophila*. *Neuron* **49**, 833–844 (2006).
20. Jefferis, G.S. *et al.* Comprehensive maps of *Drosophila* higher olfactory centers: spatially segregated fruit and pheromone representation. *Cell* **128**, 1187–1203 (2007).
21. Wong, A.M., Wang, J.W. & Axel, R. Spatial representation of the glomerular map in the *Drosophila* protocerebrum. *Cell* **109**, 229–241 (2002).
22. Marin, E.C., Jefferis, G.S., Komiyama, T., Zhu, H. & Luo, L. Representation of the glomerular olfactory map in the *Drosophila* brain. *Cell* **109**, 243–255 (2002).
23. Kohsaka, H. & Nose, A. Target recognition at the tips of postsynaptic filopodia: accumulation and function of Capricious. *Development* **136**, 1127–1135 (2009).
24. Sweeney, L.B. *et al.* Temporal target restriction of olfactory receptor neurons by Semaphorin-1a/PlexinA-mediated axon-axon interactions. *Neuron* **53**, 185–200 (2007).
25. Chang, Z. *et al.* Molecular and genetic characterization of the *Drosophila tartan* gene. *Dev. Biol.* **160**, 315–332 (1993).
26. Milán, M., Pérez, L. & Cohen, S.M. Boundary formation in the *Drosophila* wing: functional dissection of Capricious and Tartan. *Dev. Dyn.* **233**, 804–810 (2005).
27. McLaughlin, T. & O'Leary, D.D. Molecular gradients and development of retinotopic maps. *Annu. Rev. Neurosci.* **28**, 327–355 (2005).
28. Imai, T., Suzuki, M. & Sakano, H. Odorant receptor–derived cAMP signals direct axonal targeting. *Science* **314**, 657–661 (2006).
29. Walz, A., Rodriguez, I. & Mombaerts, P. Aberrant sensory innervation of the olfactory bulb in neuropilin-2 mutant mice. *J. Neurosci.* **22**, 4025–4035 (2002).
30. Taniguchi, M. *et al.* Distorted odor maps in the olfactory bulb of semaphorin 3A-deficient mice. *J. Neurosci.* **23**, 1390–1397 (2003).
31. Schwarting, G.A. *et al.* Semaphorin 3A is required for guidance of olfactory axons in mice. *J. Neurosci.* **20**, 7691–7697 (2000).
32. Schwarting, G.A., Raitcheva, D., Crandall, J.E., Burkhardt, C. & Püschel, A.W. Semaphorin 3A-mediated axon guidance regulates convergence and targeting of P2 odorant receptor axons. *Eur. J. Neurosci.* **19**, 1800–1810 (2004).
33. Imai, T. *et al.* Pre-target axon sorting establishes the neural map topography. *Science* **325**, 585–590 (2009).
34. Cutforth, T. *et al.* Axonal ephrin-As and odorant receptors: coordinate determination of the olfactory sensory map. *Cell* **114**, 311–322 (2003).
35. Kaneko-Goto, T., Yoshihara, S., Miyazaki, H. & Yoshihara, Y. BIG-2 mediates olfactory axon convergence to target glomeruli. *Neuron* **57**, 834–846 (2008).
36. Serizawa, S. *et al.* A neuronal identity code for the odorant receptor–specific and activity-dependent axon sorting. *Cell* **127**, 1057–1069 (2006).

ONLINE METHODS

Fly stocks. *GH146-Gal4* (ref. 37) and *Mz19-Gal4* (ref. 5) were used to label PNs. *Or-Gal4* lines (*Or22a-Gal4*, *Or46a-Gal4*, *Or47a-Gal4*, *Or47b-Gal4*, *Or59c-Gal4*, *Or67b-Gal4* and *Or88a-Gal4*)[24,38–41], *AM29-Gal4* (ref. 42) and *Pebbled-Gal4* (ref. 24) were used to label ORNs. The enhancer trap line *caps-Gal4* (NP3294)[18] is used to visualize Caps-expressing cells and *trn-lacZ*[25] is used to visualize Trn-expressing cells. P{GS6}10839 (*caps*) and P{GS6}10885 (*trn*) were generated by the *Drosophila* Gene Search Project (Metropolitan University)[43]. The single and double null-mutant alleles of *caps* and *trn* that we used were *caps*^{c28fs}*FRT2A*[15,18], *trn*$^{28.4}$*FRT2A*[15,25], *trn*^{Δ17}*caps*^{c28fs}*FRT2A*[15] and *trn*$^{28.4}$*caps*^{Δ1}*FRT80B*[16], as well as a small *caps* deficiency allele, *Df(3L)Exel6118. caps*^{c28fs} contains a seven–base pair deletion that results in a frame shift after the first 28 amino acids[15,18]. *trn*$^{28.4}$ carries a small deletion of *trn* gene generated by P-element excision[25]. *trn*^{Δ17}*caps*^{c28fs} was generated on the basis of the null allele *caps*^{c28fs} and carries an additional deletion covering the entire *trn* coding sequence[15]. *trn*$^{28.4}$*caps*^{Δ1} was generated on the basis of the null allele *trn*$^{28.4}$ and carries an additional deletion covering the entire *caps* coding sequence[16]. A *UAS-caps* transgene[13] inserted on the third chromosome was used for rescue and misexpression experiments. The flies that we used in the overexpression screen were previously described[12].

Clonal analysis. The MARCM method was applied as described previously[44,45]. Briefly, *caps* and/or *trn* alleles were placed *trans*-heterozygous to *Gal80* on the FRT chromosome arm[15,18]. Flipase activity caused mitotic recombination of the FRT chromosome arm such that one of the daughter cells became homozygous for *caps* or *trn* and simultaneously lost *Gal80*. This cell (and its progeny) can therefore be labeled by the *Gal4/UAS* system.

For ORN analysis, *ey-Flp* was used to induce clones in nearly half of the ORNs and *Or*-specific *Gal4* lines were used to label these clones. For PN analysis, clones were generated by *hsFlp* and labeled by *GH146-Gal4* or *Mz19-Gal4*. For generating neuroblast clones, flies were heat shocked between 24–36 h after egg laying for 1 h at 37 °C. For generating class-specific clones, flies were heat shocked during a unique time window after egg laying for 1 h at 37 °C and the clone identities were determined by the combination of *Gal4* lines used, heat shock window, neuroblast lineage and axon branching pattern. Four Caps-negative (DL1, DA1, DC3 and VA1d) and four Caps-positive (VC1, VC2, VA4 and DM1) PN classes were investigated here. *Mz19-Gal4* labels DC3 and VA1d from the anterodorsal neuroblast and DA1 from the lateral neuroblast[5]. We used *MZ19-Gal4* to analyze dendrite targeting of DC3/VA1d and DA1 by generating neuroblast clones at 24–36 h after egg laying. The other five classes were analyzed as single-cell clones using *GH146-Gal4*. To analyze DL1 PNs, we heat shocked flies between 24–36 h after egg laying; 100% of the anterodorsal PN single-cell clones generated at this time are DL1 (ref. 4). To analyze the four Caps-positive PNs in the lateral lineage, we identified a time window of clone induction (36–48 h after egg laying) in which all of the *GH146-Gal4*–positive single-cell PN clones generated from the lateral neuroblast were *caps*-positive and projected their dendrites to VA4, DM1, VC1 or VC2 glomerulus in wild-type controls (**Fig. 3d**–**g**). The axon branching pattern of VC1 in the lateral horn was uniquely identifiable among the four groups and was unchanged in *caps* mutants (**Supplementary Fig. 4**). We performed a blind test of mixing axon patterns of single-cell MARCM clones of four PN classes each with three genotypes, control, mutant and rescue. All of the VC1 PNs were identified in the blind test with 100% accuracy; the mutant VC1 samples were also validated by their partial dendrite innervation of VC1 in addition to ectopic glomeruli. These criteria allowed us to identify VC1 PNs unequivocally. The other three Caps-positive PN classes (VC2, VA4 and DM1) also had characteristic lateral horn axon branching patterns that were largely unchanged in mutants. However their axon branching patterns were more similar to each other and were not 100% identified in our blind test. Therefore, we analyzed dendrite mistargeting of these three classes together (**Fig. 3u,v**). We assigned a class to each representative image in **Figure 3l–n** on the basis of their partial innervation of VC2, VA4 or DM1. Flies were raised at 25 °C after heat shock and dissected 5–7 d after eclosion.

For analyzing DL1 single-cell misexpression during development, flies were raised at 29 °C after heat shock to increase expression level and overcome Gal80 perdurance. Flies were dissected at 12 h APF and 36 h APF at 29 °C, which are equivalent to 16 h APF and 48 h APF at 25 °C, respectively.

To determine whether the preference of mistargeting events that occur in glomerular targets of Caps-positive or negative PNs (or ORNs) is statistically significant, each experiment was tested by χ^2 on the basis of the null hypothesis that mistargeting events occur randomly in Caps-positive and negative glomeruli. P values were determined for each experiment and used to accept or reject the null hypothesis. For PN MARCM analysis, we used the *hsFlp*^{122}; *UAS–-mCD8-gfp*, *GH146-Gal4*; *UAS–mCD8-gfp*, and *caps* (and/or *trn*) *FRT2A* (or *FRT80B*) / *G80 FRT2A* (or *FRT80B*) genotypes. For ORN analysis, we used the *ey-Flp*; *UAS–mCD8-gfp*, *Or-Gal4*; *UAS–mCD8-gfp*, and *caps* (and/or *trn*) *FRT2A/G80 FRT2A* genotypes.

New transgenes. The p[*Gal4, w+*]^{GH146} enhancer trap was inserted into the 5′ upstream region of the *oaz* gene (*CG17390*). The cloned *GH146* genomic enhancer was a 12.6-kb fragment that included all of the genomic DNA between *oaz* and the upstream gene *CG17389*, as well as all *oaz* introns. The *Gal4* coding region from *pBAC-3xPDsRed-GH146-Gal4* (ref. 46) was replaced with *Gal80* to generate *pBAC-3xPDsRed-GH146-Gal80* (C.J.P. and L.L., unpublished reagent). Site-directed mutagenesis of *pBAC-3xPDsRed-GH146-Gal80* was used to introduce FseI and AvrII restriction sites flanking the *Gal80* coding region. A linker oligonucleotide was ligated into the FseI/AvrII site to generate *pBAC-3xPDsRed-GH146-MCS* with multicloning site FseI-AscI-AvrII. Mammalian optimized FLPase (FLPo, Addgene plasmid 13792)[47] was PCR amplified to include the FseI/AvrII restriction sites and cloned into *pBAC-3xPDsRed-GH146-MCS* to generate *pBAC-3xPDsRed-GH146-FLPo* (*GH146-Flp*).

The *FRT-stop-FRT* cassette, with additional *Bgl*II/NotI restriction sites, was PCR amplified from genomic DNA of UAS-*FRT-stop-FRT-shibire*^{ts} flies[48] and cloned into *pUAST–mCD8-gfp*[45] to generate *pUAST-FRT-stop-FRT-mCD8-gfp* (*UAS>stop>mCD8-gfp*). All constructs were sequence verified. Transgenic flies were generated as previously described[49].

Immunochemistry. The procedures that we used for fixation, immunochemistry and imaging were described previously[50]. For primary antibodies, we used mouse nc82 (1:30), rat antibody to N-cadherin (1:40), rat antibody to mCD8 (1:100), chicken antibody to GFP (1:300) and rabbit antibody to Caps (1:100)[13].

37. Stocker, R.F., Heimbeck, G., Gendre, N. & de Belle, J.S. Neuroblast ablation in *Drosophila* P[GAL4] lines reveals origins of olfactory interneurons. *J. Neurobiol.* **32**, 443–456 (1997).
38. Couto, A., Alenius, M. & Dickson, B.J. Molecular, anatomical, and functional organization of the *Drosophila* olfactory system. *Curr. Biol.* **15**, 1535–1547 (2005).
39. Fishilevich, E. & Vosshall, L.B. Genetic and functional subdivision of the *Drosophila* antennal lobe. *Curr. Biol.* **15**, 1548–1553 (2005).
40. Komiyama, T., Carlson, J.R. & Luo, L. Olfactory receptor neuron axon targeting: intrinsic transcriptional control and hierarchical interactions. *Nat. Neurosci.* **7**, 819–825 (2004).
41. Kreher, S.A., Kwon, J.Y. & Carlson, J.R. The molecular basis of odor coding in the *Drosophila* larva. *Neuron* **46**, 445–456 (2005).
42. Endo, K., Aoki, T., Yoda, Y., Kimura, K. & Hama, C. Notch signal organizes the *Drosophila* olfactory circuitry by diversifying the sensory neuronal lineages. *Nat. Neurosci.* **10**, 153–160 (2007).
43. Toba, G. *et al.* The gene search system. A method for efficient detection and rapid molecular identification of genes in *Drosophila melanogaster*. *Genetics* **151**, 725–737 (1999).
44. Wu, J.S. & Luo, L. A protocol for mosaic analysis with a repressible cell marker (MARCM) in *Drosophila*. *Nat. Protoc.* **1**, 2583–2589 (2006).
45. Lee, T. & Luo, L. Mosaic analysis with a repressible cell marker for studies of gene function in neuronal morphogenesis. *Neuron* **22**, 451–461 (1999).
46. Berdnik, D., Fan, A.P., Potter, C.J. & Luo, L. MicroRNA processing pathway regulates olfactory neuron morphogenesis. *Curr. Biol.* **18**, 1754–1759 (2008).
47. Raymond, C.S. & Soriano, P. High-efficiency FLP and PhiC31 site-specific recombination in mammalian cells. *PLoS One* **2**, e162 (2007).
48. Stockinger, P., Kvitsiani, D., Rotkopf, S., Tirián, L. & Dickson, B.J. Neural circuitry that governs *Drosophila* male courtship behavior. *Cell* **121**, 795–807 (2005).
49. Schuldiner, O. *et al.* piggyBac-based mosaic screen identifies a postmitotic function for cohesin in regulating developmental axon pruning. *Dev. Cell* **14**, 227–238 (2008).
50. Wu, J.S. & Luo, L. A protocol for dissecting *Drosophila melanogaster* brains for live imaging or immunostaining. *Nat. Protoc.* **1**, 2110–2115 (2006).